Cellular/Molecular

Phosphorylation of RPT6 Controls Its Ability to Bind DNA and Regulate Gene Expression in the Hippocampus of Male Rats during Memory Formation

Kayla Farrell,[1] Aubrey Auerbach,[2] Madeline Musaus,[3] Shaghayegh Navabpour,[4] Catherine Liu,[1] Yu Lin,[5] Hehuang Xie,[3,5,6] and Timothy J. Jarome[1,3,4]

[1]Departments of School of Animal Sciences, [2]Biological Sciences, [3]School of Neuroscience, [4]Translational Biology, Medicine, and Health Graduate Program, Virginia Polytechnic Institute and State University, Blacksburg 24060, Virginia, [5]Department of Biomedical Sciences and Pathobiology, Virginia-Maryland College of Veterinary Medicine, Blacksburg 24060, Virginia, and [6]Fralin Life Science Institute at Virginia Tech, Blacksburg 24060, Virginia

Memory formation requires coordinated control of gene expression, protein synthesis, and ubiquitin–proteasome system (UPS)-mediated protein degradation. The catalytic component of the UPS, the 26S proteasome, contains a 20S catalytic core surrounded by two 19S regulatory caps, and phosphorylation of the 19S cap regulatory subunit RPT6 at serine 120 (pRPT6-S120) has been widely implicated in controlling activity-dependent increases in proteasome activity. Recently, RPT6 was also shown to act outside the proteasome where it has a transcription factor-like role in the hippocampus during memory formation. However, little is known about the proteasome-independent function of "free" RPT6 in the brain or during memory formation and whether phosphorylation of S120 is required for this transcriptional control function. Here, we used RNA-sequencing along with novel genetic approaches and biochemical, molecular, and behavioral assays to test the hypothesis that pRPT6-S120 functions independently of the proteasome to bind DNA and regulate gene expression during memory formation. RNA-sequencing following siRNA-mediated knockdown of free RPT6 revealed 46 gene targets in the dorsal hippocampus of male rats following fear conditioning, where RPT6 was involved in transcriptional activation and repression. Through CRISPR-dCas9-mediated artificial placement of RPT6 at a target gene, we found that RPT6 DNA binding alone may be important for altering gene expression following learning. Further, CRISPR-dCas13-mediated conversion of S120 to glycine on RPT6 revealed that phosphorylation at S120 is necessary for RPT6 to bind DNA and properly regulate transcription during memory formation. Together, we reveal a novel function for phosphorylation of RPT6 in controlling gene transcription during memory formation.

Key words: **CRISPR; hippocampus; memory; proteasome; RPT6; transcription**

Significance Statement

The role of the proteasome subunit RPT6, particularly when phosphorylated at serine 120 (pRPT6-S120), has been extensively studied in the context of proteasome-mediated protein degradation, but its role in regulating gene expression during memory formation has not been explored. This study identifies gene targets of RPT6 during memory formation and reveals that the presence of RPT6 alone at DNA may cause changes in gene expression. Further, we found that pRPT6-S120 was necessary for DNA binding and transcriptional regulation during memory formation. Considering the popularity of proteasome-inhibiting drugs, these data are noteworthy for the neuroscience community as they demonstrate a clear role for proteasome-independent RPT6 in transcriptional regulation of gene expression during memory formation, which is dysregulated when RPT6 is manipulated.

Received Aug. 1, 2023; revised Oct. 31, 2023; accepted Nov. 29, 2023.

Author contributions: K.F. and T.J.J. designed research; K.F., A.A., M.M., S.N., and C.L. performed research; K.F., Y.L., H.X., and T.J.J. analyzed data; K.F. wrote the paper.

We thank Shannon Mauro for technical assistance.

This work was supported by National Institutes of Health grants MH122414, MH131587, MH120498, MH120569, MH123742, AG071523, and AG079292 to T.J.J.

The authors declare no competing financial interests.

Correspondence should be addressed to should be addressed to Timothy J. Jarome at tjjarome@vt.edu.

https://doi.org/10.1523/JNEUROSCI.1453-23.2023

Introduction

Memory formation relies on cells to undergo a series of changes in gene expression, de novo protein synthesis, and protein degradation (Bourtchouladze et al., 1998; Martin et al., 2021; Weber Boutros et al., 2022). In terms of the latter, one mechanism that is highly studied for its role during fear memory formation is the ubiquitin–proteasome system (UPS), the major degradation pathway in cells (Hershko and Ciechanover, 1998;

Patrick et al., 2023). The UPS utilizes a small regulatory protein known as ubiquitin to label proteins for degradation by the 26S proteasome complex. This complex is comprised of two parts, a 20S catalytic core which is barrel-shaped and contains α and β subunits, and two 19S caps, which act as a gatekeeper to only allow proteins labeled for degradation to enter. The 19S caps contain RPN and RPT proteins, the latter of which are ATPases and control gate opening (Lander et al., 2012). One RPT protein, RPT6, has been widely studied, as phosphorylation of RPT6 at serine 120 (pRPT6-S120) has been shown to regulate proteasome activity, synaptic strength, and dendritic spine growth in vitro (Zhang et al., 2007; Djakovic et al., 2009, 2012; Bingol et al., 2010; Hamilton et al., 2012) and proteasome activity in vivo (Scudder et al., 2021). Interestingly, proteasome-independent "free" RPT6 has also been found to play a role in epigenetic regulation in yeast (Gonzalez et al., 2002; Ezhkova and Tansey, 2004) and during memory formation in the hippocampus of rats (Jarome et al., 2021; Farrell et al., 2022), though the importance of phosphorylation state in this process has not been explored.

We previously showed that RPT6 is a binding partner of the epigenetic regulator, monoubiquitination of histone H2B at lysine 120 (H2BubiK120) in the dorsal hippocampus of male and female rats during fear memory formation (Jarome et al., 2021; Farrell et al., 2022). Surprisingly, we also found that females, but not males, require UPS-mediated protein degradation in the hippocampus for fear memory formation (Martin et al., 2021). Together, these studies suggest that RPT6 may regulate memory formation outside of the proteasome in the hippocampus of males but within the proteasome in females. However, the target genes of RPT6 during memory formation remain unknown, and it is unclear if RPT6 regulates both transcriptional activation and repression. Further, it is unknown how RPT6 binds DNA and whether phosphorylation of S120 is important for this process.

The objective of this study was to better characterize the epigenetic role of RPT6 in the hippocampus during memory formation. Due to previous evidence of RPT6 acting in an epigenetic capacity and the importance of pRPT6-S120 for proteasome activity, we hypothesized that pRPT6-S120 functions independently of the proteasome to bind DNA and regulate gene expression during memory formation. We tested this hypothesis in four experiments. In experiment 1, we knocked down *Psmc5*, the RPT6-coding gene, in the hippocampus and then conducted RNA-sequencing (RNA-seq) in control and *Psmc5* knockdown animals 1 h after training to identify RPT6 gene targets during memory formation in the hippocampus. In experiment 2, we artificially placed RPT6 at the promoter of *Egr2*, an immediate early gene identified in our RNA-seq experiment, in the hippocampus to determine if RPT6 alone at DNA can induce changes in gene expression following weak training. In experiments 3 and 4, we used the CRISPR-dCas13 system to remove the phosphorylation site at S120 in the hippocampus to determine if RPT6 could bind DNA regardless of phosphorylation status at S120. Through these experiments, we determined that RPT6 (1) regulates increases and decreases in gene expression following learning, (2) placement at DNA may affect transcription, and (3) must be phosphorylated at S120 to bind DNA. Together, these findings provide the first evidence that RPT6 controls gene upregulation and downregulation and that phosphorylation of RPT6 at S120 controls the ability of proteasome-independent RPT6 to bind DNA and properly regulate gene expression in the hippocampus during memory formation.

Materials and Methods

Subjects. A total of 83 male Sprague Dawley rats, aged 8–9 weeks (Envigo), were used for these experiments. Animals were housed two per cage with free access to water and rat chow under a 12:12-h light/dark cycle, with experiments being conducted during only the light hours of the cycle. All procedures were approved by the Virginia Polytechnic Institute and State University Animal Care and Use Committee (protocol #20-233) and done in accordance with the National Institutes of Health ethical guidelines.

Accell siRNA. Targeted knockdown of *Psmc5* in the CA1 region of the dorsal hippocampus was completed using Accell short interfering RNA as previously described (Farrell et al., 2022). Accell SMARTpool siRNA targeting *Psmc5* (#E-096860-00-0005 Dharmacon) or scrambled control (#D-001910-10-05 Dharmacon) were resuspended immediately prior to surgery. Accell siRNA delivery medium was used to resuspend a 100 μM stock of Accell SMARTpool siRNA to a final concentration of ~10 μM.

CRISPR/dCas13 gRNA plasmid cloning. The CRISPR/dCas13 plasmids were cloned following previously described procedures (Cox et al., 2017; Melfi et al., 2020; Farrell et al., 2023). Briefly, a guide RNA (gRNA) was designed to target the *Psmc5* mRNA sequence coding for serine at position 120 of the RPT6 protein. The gRNA was 50 bp long and contained a mismatch at position 34 from 5′ at the first adenosine coding for serine. The backbone plasmid (pC0043-PspCas13b crRNA backbone; #103854 Addgene) was digested with Bbsi (CACC; #R0539S New England Biolabs). The complement sequence to the remaining sticky ends was added to the 5′ end of the gRNA sequence for directional cloning in addition to a 5′ phosphate. The gRNA oligos were resuspended in annealing buffer (10 mM Tris, pH 7.5–8.0, 50 mM NaCl, and 1 mM EDTA), combined in equal parts, and then heated to 95°C for 2 min before being cooled to room temperature in order to anneal. The backbone plasmid was then digested with Bbsi, agarose gel purified using the Zymoclean Large Fragment DNA recovery kit (#D4045 Zymo Research), treated with shrimp alkaline phosphatase (#M0371S New England Biolabs) at 37°C for 30 min, purified using the GeneJET PCR purification kit (#K0701 Thermo Fisher Scientific), and then ligated with the gRNA DNA fragment by T4 ligase (#BP80995 Thermo Fisher Scientific). Following ligation, One Shot TOP10 Chemically Competent *E. coli* (#C404003 Invitrogen) was used to transform the ligation reaction, and then positive clones were confirmed through sequencing with the pUC-M13 reverse primer (#N53002 Thermo Fisher Scientific). The CMV-dPspCas13b-GS-ADAR2DD(E488Q/T375G)-delta-984-1090 (#103871 Addgene) plasmid was used for editing. NucleoBond Xtra Midi Plus EF kit (#740422.10 Macherey-Nagel) was used following the manufacturer's instruction to generate a bulk amount of plasmid.

CRISPR-dCas9-RPT6-FLAG and gRNA cloning. The dCas9-KRAB-MeCP2 (#110821 Addgene) plasmid was altered to generate the dCas9-RPT6-FLAG plasmid. A vector containing a portion of the sequence coding for Cas9m4, the full endogenous *Rattus norvegicus Psmc5* coding region after the first methionine, and the cut site sequences for AgeI and AscI was ordered from Addgene. The plasmid was resuspended to a 100 μM stock in IDTE buffer (10 mM Tris, 0.1 mM EDTA). One Shot TOP10 Chemically Competent *E. coli* was used to transform 100 ng of the plasmid and then the NucleoBond Xtra Midi Plus EF kit was used following the manufacturer's instruction to generate a bulk amount for use in cloning. The RPT6-coding plasmid was digested with AscI (#R0558S New England Biolabs) and AgeI (#R3552S New England Biolabs), and then the fragment containing the RPT6-coding portion was agarose gel purified using the Zymoclean Large Fragment DNA recovery kit. The dCas9-KRAB-MeCP2 was also digested with AscI and AgeI, which allowed for the removal of the sequence coding for KRAB-MeCP2 but the retention of the plasmid coding for Cas9m4. The RPT6-coding fragment and the digested dCas9 plasmid were then ligated by T4 ligase and transformed into One Shot TOP10 Chemically Competent *E. coli*. Positive clones were confirmed through sequencing

with a forward (GACGCTAACCTCGATAAGGTGCTTTC) and reverse (GAACAAACGACCCAACACCCG) primer, and then NucleoBond Xtra Midi Plus EF kit was used following the manufacturer's instruction to generate a bulk amount of plasmid.

Two PCR reactions using Phusion Green Hot Start II High-Fidelity PCR Master Mix (#F566S Thermo Fisher Scientific) were then conducted using the dCas9-RPT6 plasmid to remove the RPT6 stop codon and add sequences coding for SV40 nuclear localization signal (NLS) followed by 3× FLAG on the 3′ end of the RPT6-coding insert to visualize the plasmid. The first PCR was conducted using the same forward primer (GACGCTAACCTCGATAAGGTGCTTTC), a unique reverse primer (CACCTTCCGTTTCTTCTTTGGGCTTGATCCAGAGCCCTTCCAA AGCTTCTTGATGGACATG), which excluded the sequence coding for the RPT6 stop codon and added a 3′ tail sequence coding for SV40 NLS, and the following protocol: 98°C for 1 min, then 98°C for 30 s, 58°C for 30 s, followed by 72°C for 2 min (32 repeats), then 72°C for 5 min, and finally held at 4°C. The PCR product was agarose gel purified using the Zymoclean Large Fragment DNA recovery kit and then used for a subsequent PCR using the same forward primer, another unique reverse primer (TTACTAACCGGTAGGGATCGAATTCTTTCACTTATCGT CATCGTCTTTGTAATCAATATCATGATCCTTGTAGTCTCCGTCGT GGTCCTTATAGTCTGAGGCTTCCACCTTCCGTTTCTTCTTTGG) which added a 3′ tail sequence coding for 3× FLAG with AscI and AgeI, re-purified with the GeneJET PCR purification kit, and then ligated into the digested dCas9-KRAB-MeCP2 backbone used above by T4 ligase. The ligation reaction was transformed into One Shot TOP10 Chemically Competent *E. coli* and then positive clones were confirmed through sequencing with the same forward primer (GACGCTAACCTCGAT AAGGTGCTTTC), a new forward primer (CGGTTCTTCACGGCT GGAG), and a reverse (GAACAAACGACCCAACACCCG) primer. The NucleoBond Xtra Midi Plus EF kit was then used following the manufacturer's instruction to generate a bulk amount of plasmid for use in experiments. The dCas9-RPT6-FLAG plasmid was submitted to Addgene (#205416).

CRISPR gRNA targeting the DNA region within 300 bp of the *Egr2* promoter were designed using CRISPOR CRISPR Design Tool as previously described (Jarome et al., 2021). The sequence (AGACCC GGGCGGTTGTCCAC) was inserted into the 293-T backbone and then cloned into the CRISPR gRNA vector (#44248 Addgene). One Shot TOP10 Chemically Competent *E. coli* was used for transformation, and then positive clones were confirmed through sequencing with a reverse primer (ATGCATGGCGGTAATACGGT). Cells were then grown in LB broth with ampicillin and purified with the NucleoBond Xtra Midi Plus EF kit following the manufacturer's instruction to generate a bulk amount of plasmid.

Rat B35 neuroblastoma cell culture. Cell culture of rat B35 neuroblastoma cells was done using previously described procedures (Jarome et al., 2021). Briefly, the cells (#CRL-2754 ATCC) were cultured in Dulbecco's Modified Eagle's Medium (DMEM; #30-2002 ATCC) which was supplemented with 0.1% Penicillin/Streptomycin (#15070063 Gibco) and 10% Fetal Bovine serum (#35-016-CV Corning). When cells reached 70–90% confluency, they were exposed to 0.05% Trypsin-EDTA (1×; #25300054 Gibco) and transferred to a six-well dish containing 2 ml of DMEM-based media in a 1:6 ratio. After 24 h, transfection was completed with Lipofectamine 3000 reagent (#L3000001 Invitrogen) following the manufacturer's instructions. First, DMEM-based media was removed, cells were washed with DPBS (#14190144 Gibco), and then pre-warmed Opti-MEM media (#31985070 Gibco) was added to each well. Plasmids were prepared by mixing with Lipofectamine 3000 reagent and Opti-MEM media following the manufacturer's instructions. The plasmid–lipofectamine mixture was then added to the cells, which were incubated in a NAPCO series 8000 Water Jacket CO_2 incubator (model 3586) for 48 h post transfection. Following the 48 h incubation, whole-cell protein lysates were isolated from each well individually using the method described below in the Whole-cell protein extraction section.

Stereotaxic infusions. CRISPR plasmids or Accell siRNA were infused cranially by stereotactic surgery according to previously described methods (Jarome et al., 2021; Farrell et al., 2022). Briefly, animals were anesthetized with 1.5–4% isoflurane in 100% O_2 before receiving a bilateral infusion of either CRISPR plasmids or Accell SMARTpool siRNA into the CA1 region of the dorsal hippocampus using the following coordinates relative to bregma: AP −3.6 mm, ML ± 1.7 mm, DV −3.6 mm. In the case of CRISPR plasmid infusion, in vivo JetPEI Transfection Reagent (#101000040 Polyplus, New York, NY) was used as in our previous studies (Jarome et al., 2021; Martin et al., 2021; Farrell et al., 2023). The linear actuator used for infusion was set to a constant rate of 0.1 µl per minute for a total volume of 1 µl per side. When animals received siRNA infusion, they were handled for 4 consecutive days prior to surgery and were allowed 5 d to recover after surgery before behavioral training was conducted. When animals received CRISPR plasmid infusion, they were allowed 7 d to recover, after which they were handled for 4 consecutive days, and then behavioral training was conducted 28 d after surgery.

Behavior procedures. Rats were trained to a contextual fear conditioning paradigm as previously described (Jarome et al., 2021). For standard contextual fear conditioning, rats were placed in a Habitest chamber (novel context) for 7 min, during which time three unsignaled footshocks were administered (1 mA, 2 s, 120 s ITI). For weak contextual fear conditioning (Jarome et al., 2021), rats were placed in a Habitest chamber (novel context) for 5 min, during which time only the first two unsignaled footshocks were administered (0.6 mA, 2 s, 120 s ITI). For testing, animals were placed back into the same Habitest chamber without any footshock presentations for 5 min. FreezeFrame software was used for live scoring of freezing behavior, and videos were stored for later use. A freezing threshold of 2 was used to calculate average percent time freezing during training and testing for all animals.

Experimental design. In experiment 1, male rats received a bilateral infusion of either nontargeting control (Scr-siRNA) Accell siRNA or Accell siRNA targeting *Psmc5*, the coding gene for RPT6, into area CA1 of the dorsal hippocampus. Animals were handled for 4 d prior to surgery, and 5 d after surgery, rats in a training group were trained to standard contextual fear conditioning. Animals were euthanized 1 h after training, and naïve rats were euthanized at a similar timepoint. The CA1 region of the dorsal hippocampus was dissected. RNA was collected from one hemisphere of CA1 tissue and used for RNA-seq and qPCR. The other hemisphere of CA1 tissue was used for ChIP analysis. Group sizes were as follows: Scr-siRNA naïve = 5, Scr-siRNA trained = 5, and *Psmc5*-siRNA trained = 5. As fear conditioning causes a downregulation in *Psmc5* gene expression in the hippocampus (Jarome et al., 2021), separate groups of rats received bilateral infusions of Scr-siRNA or *Psmc5*-siRNA into the CA1 region and were euthanized 5 d later for confirmation of *Psmc5* knockdown.

In experiment 2, male rats received a bilateral infusion of either *Egr2* gRNA alone (control) or *Egr2* gRNA with the CRISPR-dCas9-RPT6-FLAG plasmid (*Egr2* + dCas9-RPT6) into area CA1 of the dorsal hippocampus. Animals were handled four times between 7 and 14 d after surgery, and then 28 d after surgery, rats were trained to weak contextual fear conditioning. Animals were euthanized 1 h after training, and naïve animals were euthanized at a similar timepoint. The CA1 region of the dorsal hippocampus was collected. RNA for qPCR analysis of gene expression was collected from one hemisphere of CA1 tissue (control naïve $n = 8$, control trained $n = 7$, *Egr2* + dCas9-RPT6 trained $n = 7$), and the other tissue was used for ChIP analysis [control naïve $n = 8$, control trained $n = 7$ ($n = 6$ for *Egr2* 3′ UTR), *Egr2* + dCas9-RPT6 trained $n = 7$]. Immunohistochemistry was conducted with the brain of one animal injected with the dCas9-RPT6-FLAG plasmid.

In experiments 3–4, a gRNA targeting S120 on RPT6 was designed and then verified through transfection into rat B35 neuroblastoma cells. Cells were transfected with dCas13-ADAR2DD plasmid alone (control) or gRNA targeting S120 and dCas13-ADAR2DD plasmid (Cas13-S120), and then protein was collected and used for Western blot (control $n = 7$, Cas13-S120 $n = 8$). Then, male rats received a bilateral infusion of either gRNA targeting S120 and dCas13b-ADAR2DD plasmids (RPT6 + Cas13

trained) or dCas13b-ADAR2DD plasmid alone (control) into area CA1 of the dorsal hippocampus. Animals were handled four times between 7 and 14 d after surgery, and then 28 d after surgery, rats were trained to standard contextual fear conditioning. In experiment 3, animals were euthanized 1 h later with naïve animals euthanized at a similar timepoint, and the CA1 region of the dorsal hippocampus was collected. One hemisphere of CA1 tissue was used for qPCR analysis of gene expression and the other used for ChIP analysis. Group sizes were as follows: control naïve = 6, control trained = 6, and RPT6 + Cas13 trained = 6. In experiment 4, all animals were trained, and then 24 h later, they were placed back into the chamber for testing. One hour after testing, animals were euthanized, and the CA1 region of the dorsal hippocampus was collected. One hemisphere of CA1 tissue was used for proteasome activity assay. Group sizes were as follows: Cas13 control = 8 and RPT6 + Cas13 = 8.

Tissue collection. Hippocampal tissue was collected by first overdosing rats on isoflurane in a necrosis chamber, followed by decapitation and rapid brain removal. Brains were immediately frozen on dry ice following removal. Animals in an experimental training group were euthanized 1 h after the training session, and naïve animals were euthanized at the same time. Animals that underwent testing were euthanized 1 h after the testing session. Both hemispheres of the CA1 region of the hippocampus were dissected on dry ice and then stored at −80°C until needed.

RNA isolation and cDNA synthesis. RNA extraction and cDNA synthesis were completed as previously described (Farrell et al., 2022). Briefly, RNA was extracted from one hemisphere of the CA1 region using the RNeasy Mini kit (#74104 Qiagen). The RNA concentration and quality were measured using the Take3 (BioTek) as well as a Nanodrop. The iScript cDNA synthesis kit (#1708890 Bio-Rad) was then used for cDNA synthesis with 200 ng of normalized RNA.

RNA-sequencing. RNA extracted from dorsal CA1 tissue collected from fear-conditioned rats 1 h after training or from naïve animals at a similar timepoint was used for whole-transcriptome RNA-seq performed at the Genomics Sequencing Center at Virginia Tech. First, Illumina's TruSeq Stranded mRNA HT Sample Prep Kit (#RS-122-2103 Illumina) was used to convert RNA into a strand-specific library, which was used for cluster generation and sequencing on Illumina's NovaSeq 6000. PCR was used to enrich the libraries by 14 cycles which was then validated using Agilent TapeStation and quantitated by qPCR. Individually indexed cDNA libraries were pooled and sequenced on NovaSeq 6000 S1 150 cycle PE to achieve a minimum of 25 million reads/sample. The BCL files were converted to FASTQ files, adapters trimmed and demultiplexed using bcl2fastq Conversion Software. Data were submitted to the Gene Expression Omnibus (GEO) repository (accession #GSE237868).

RNA-seq data analysis. RNA-seq data analysis was performed using in-house scripts. Trim Galore (v0.6.5) was used to filter short reads, low-quality reads, and trim adapter sequences from raw reads. Clean reads were mapped to the *Rattus norvegicus* genome (v6.0.99) and quantified using STAR (v2.7.3a). The raw counts were employed to identify differentially expressed genes by R package DESeq2 (v1.36.0). Genes with larger than 1.2-fold change and adjusted *p*-value less than 0.05 were considered significant. The results were visualized using R package EnhancedVolcano (v1.14.0) and ComplexHeatmap (v2.12.1).

Quantitative RT-PCR. Quantitative PCR amplifications of cDNA or ChIP DNA were performed as previously described (Farrell et al., 2022) using SsoAdvanced Universal SYBR Green Supermix (#1725274 Bio-Rad). The Bio-Rad CFX96 Real-Time System was used for quantitative PCR with the following protocol: 98°C for 3 min, then 98°C for 10 s, followed by 60°C for 40 s (39 repeats), 55–95°C for 0.5°C/cycle, followed by a melt curve starting at 55°C for 10 s (81 repeats), and then held at 4°C. The following rat primers were used for cDNA amplification: *Egr2* (For-AAGGCCGTAGACAAAATCCCA, Rev-CCAGCCACTCC GTTCATCTG) and *Gapdh* (For-GGGCTGAGTTGGGATGGGGACT, Rev-ACCTTTGATGCTGGGGCTGGC). The *Gapdh* expression level was used as an internal control for normalization, and then the comparative Ct method was used to analyze all data.

Antibodies. Antibodies used for Western blotting include RPT6 (1:5000, #ab178681 Abcam) and pRPT6-S120 (1:1,000, #12880 Signalway Antibody LLC). Antibodies used for ChIP include RPT6 (#ab178681 Abcam), pRPT6-S120 (#12880 Signalway Antibody LLC), and H2BubiK120 (#5546 Cell Signaling). Antibodies used for immunohistochemistry include 3× FLAG/DDDDK tag (1:500, #ab205606 Abcam).

Chromatin immunoprecipitation. The methods used for chromatin immunoprecipitation (ChIP) have been described previously (Farrell et al., 2022). First, one hemisphere of CA1 tissue was chopped into small pieces in 1× PBS with protease inhibitor cocktail (#P8340, MilliporeSigma) and 1 µl/ml phosphatase inhibitor cocktail (#524625, MilliporeSigma). PBS was removed, and then tissue was fixed in PBS with 1% formaldehyde for 10 min at 37°C. Following fixation, glycine (2.5 M) was added to quench the reaction, and then the fixed tissue was washed 5 times in PBS and 1 time in PBS with inhibitors. Tissue was then homogenized in hypotonic buffer (10 mM KCl, 20 mM HEPES, 1 mM MgCl, 1 mM DTT) with protease inhibitors followed by centrifugation 1350 × *g* for 10 min at 4°C. The supernatant was discarded, and the remaining pellets (nuclei) were resuspended in ChIP sonication buffer (1× TE with 1% SDS) with protease inhibitors. Chromatin was sheared to ∼400–500 bp using the QSonic 800R2 Sonicator with 55% amplitude and 20 s pulse for 30 min, and then samples were centrifuged at 20,000 × g for 10 min at 4°C. The supernatant (DNA) was collected, DNA concentration was measured using a nanodrop, the DNA amount was normalized by dilution with TE buffer and 2× RIPA buffer (2× PBS, 1% sodium deoxycholate, 2% NP-40%, 0.2% SDS) with 2× proteasome inhibitors, and then samples were combined with Magna ChIP Protein A/G magnetic beads (#16-663 Millipore). Immunoprecipitations were carried out at 4°C overnight with primary antibody (anti-H2BubiK120, RPT6, or pRPT6-S120) or no antibody (control). The following morning, the resulting immune complexes were washed on a magnetic rack with low salt buffer (20 mM Tris, pH 8.0%, 0.1% SDS, 1% Triton X-100, 2 mM EDTA, 150 mM NaCl), high salt buffer (20 mM Tris, pH 8.1%, 0.1% SDS, 1% Triton X-100, 500 mM NaCl, 1 mM EDTA), LiCl immune complex buffer (0.25 M LiCl, 10 mM Tris, pH 8.1%, 1% deoxycholic acid, 1% IGEPAL-CA630, 500 mM NaCl, 2 mM EDTA), and twice with TE buffer. Immune complexes were extracted through two final washes with TE containing 1% SDS and sodium bicarbonate, and then samples were heated at 65°C overnight to reverse protein–DNA cross-links. Proteinase K digestion (100 µg; 2 h at 37°C) was used to destroy proteins in the sample, and then DNA was isolated through phenol/chloroform/isoamyl alcohol followed by ethanol precipitation. DNA was then used for quantitative real-time PCR with the following primers specific to the rat *Egr2* promoter (For-GAAAGTCTCGGAGAACCGGAA, Rev-CCAATTTGCATACGGGCTTGG) and 3′ UTR (For-GCCATCTC AGCCCTTAAGCA, Rev-CGACATTGCACTTCCGTTCG). Data not shown used the following primers specific to the rat *Egr2* promoter (For-CACCGGCAGCGAATCGT, Rev-CCTGGTAGCTTTTGCCGGT), Exon I (For-CTCTACCCGGTGGAAGACCT, Rev-CTCCAGCCAC TCCGTTCATC) or Exon II (For-CTACCCCCTACAATCCGCAC, Rev-GTGAGAACCTCCTGTCGCAA) regions. Following qPCR, data were analyzed by taking the cumulative fluorescence for each amplicon as a percentage of the input fraction and then taking that value as a fold change of the control group.

Immunohistochemistry. Immunohistochemistry was conducted as previously described (Farrell et al., 2023). During tissue collection, brains were placed in 4% paraformaldehyde 4°C for 24 h. Following the 24 h incubation, brains were removed from the 4% paraformaldehyde, placed in ice-cold 1× PBS, and stored at 4°C until ready for use. A vibratome was used to collect slices (∼45–50 µM) throughout the CA1 region of the

hippocampus, which were fixed with 4% paraformaldehyde and then washed with PBS. Antigen retrieval was done with boiling citric acid, and then slices were washed in PBS, blocked for 1 h in blocking buffer (4% normal goat serum, 4% normal donkey serum, and 3% Triton X in PBS), and then incubated in 3× FLAG/DDDDK tag (1:500) overnight at 4°C. Slices were then washed with PBS, incubated in Alexa Fluor 488 (1:500, #111-545-003 Jackson Immuno Research) secondary antibody for 2 h, rinsed in PBS, and then mounted on slides. VectaSheild Mounting Medium with DAPI (#H-1200 Vector Laboratories) was used to stain cell nuclei, and images were taken on a Nikon Eclipse Ci-L microscope (Nikon) and adjusted using Image J.

Whole-cell protein extraction. Forty-eight hours after transfection, Opti-MEM containing plasmids was removed, and cells were washed with DPBS. Whole-cell lysis buffer (10 mM HEPES, 1.5 mM $MgCl_2$, 10 mM KCl, 0.5 mM DTT, 0.5% IGEPAL, 0.02% SDS, 70 mM NEM, 1 µl/ml protease inhibitor cocktail, 1 µl/ml phosphatase inhibitor cocktail) was added to each well and incubated at 4°C for 5–10 min. Following incubation, individual cell populations (each well) were homogenized using a Teflon homogenizer. For experiments using protein from tissue, one hemisphere of CA1 tissue was homogenized in whole-cell lysis buffer using a Teflon homogenizer. All homogenates were centrifuged at 10,000 × g for 10 min at 4°C, supernatant was collected, and then protein concentration was measured using the Bio-Rad DC protein assay.

Western blot. Western blot was conducted as previously described (Farrell et al., 2023). Briefly, normalized proteins (10 µg) were separated on a 7% polyacrylamide gel with a 4% stacking gel and then transferred onto an Immobilon-FL membrane using the turbo transfer system (Bio-Rad). Membranes were then washed in TBS + 0.1% Tween-20 (TBSt), blocked in a 50:50 LiCOR blocking buffer (50% LiCOR TBS blocking buffer and 50% TBSt) for 1 h at room temperature, and then incubated in anti-pRPT6-S120 primary antibody at 4°C overnight. After overnight incubation, membranes were washed in TBSt for 10 min three times, incubated in a Goat anti-Rabbit secondary antibody (1:40,000, # 926-32211 LiCOR) for 45 min, and then washed in TBSt for 10 min twice more before a final rinse with TBS. Membranes were then imaged using the Odyssey Fc near infrared system (LiCOR). After development with anti-pRPT6-S120, membranes were stripped by incubating in 0.2 N NaOH for 10 min, and then they were washed with TBSt for 15 min twice, re-blocked for 1 h, and incubated in anti-RPT6 primary antibody at 4°C overnight. The mean pixel density was calculated for each sample using Image Studio version 5.2, and then pRPT6-S120 levels were normalized to total RPT6 levels, which acted as a loading control, and expressed as a percentage of the control group.

Proteasome activity assays. Proteasome activity assays were conducted as previously described (Jarome et al., 2021). Briefly, using a 96-well plate, normalized samples (10 µg) were diluted with MilliQ H_2O and mixed with reaction buffer (250 mM HEPES, pH 7.5, 5 mM EDTA, 0.5% NP-40%, 0.01% SDS, 5 mM ATP). Then, fluorogenic peptides Suc-Leu-Leu-Val-Thy-AMC (Suc-LLVY; #BML-P802-0005 Enzo Life Sciences), Z-Leu-Leu-Glu-AMC (Z-LLE; #ZW9345-0005 Enzo Life Sciences), or Bz-Val-Gly-Arg-AMC (Bz-VGR; #BW9375-0005 Enzo Life Sciences) were added to each sample at a concentration of 10 µM to assess chymotrypsin-like activity, peptidyl-glutamyl-peptide-hydrolyzing activity, or trypsin-like activity, respectively. Each reaction was incubated at 37°C for 2 h in a monochromatic plate reader (Synergy H1; BioTek), during which time fluorescence was monitored at 360 (excitation)/460 (emission). An AMC standard curve was generated using protein-free blanks, and the scans with peak levels of fluorescent signaling were used for statistical analysis. The percentage change in relative fluorescent units (RFU) is shown relative to the control group.

Protein immunoprecipitation. Protein immunoprecipitation was conducted using previously described methods (Jarome et al., 2021). Briefly, normalized whole-cell protein extracts (5 µg) were diluted in PBS with 0.01% Tween-20. Dilute samples were incubated with primary antibody (RPT6) or control (no antibody) overnight at 4°C. The following day, pierce magnetic protein A/G beads (Thermo Fisher) were washed with PBS with 0.01% Tween-20 and then mixed with the samples. The mixture was incubated with over-end mixing for 1 h at 4°C, and then samples were washed three times in PBS with 0.01% Tween-20. Immunoprecipitates were eluted by heating samples at 800 rpm for 5 min at 95°C in 1× sample buffer, and then the eluted precipitates were loaded onto 7% SDS-PAGE, exposed to primary antibody (RPT6 or pRPT6-S120), and imaged as described above in the "Western blot" section.

Statistical analyses. Data are presented as mean with standard error, with scatter plots to identify individual samples (except in line graphs). Sample size was chosen for a large effect size based on prior work from our lab using similar methods (Jarome et al., 2021; Farrell et al., 2022). Data were tested for normality, deemed parametric and analyzed in Prism software (GraphPad Software) using one- or two-way analysis of variance (ANOVA) and Tukey's Honest Significant Difference *post hoc* tests or one- or two-tailed *t* tests as indicated in the manuscript text. Nonparametric data were analyzed with Mann–Whitney *U* test. Simple linear regression with 95% confidence bands of the best-fit line was conducted for correlational analyses. Outliers were defined as data points falling two or more standard deviations from the group mean and were removed based on individual antibodies or regions of amplification rather than excluding data from an entire dataset for meeting outlier criteria on one individual, independent analysis. One outlier was identified and removed from the control trained group during the ChIP analysis for RPT6 binding at the 3′ UTR of *Egr2* in experiment 2. No other outliers were identified in the main experiments, but following the compilation of data for correlational analysis, there was one outlier removed from the control naïve correlation, two removed from the control trained correlation, and one removed from the treatment trained correlation.

Results

RPT6 regulates gene expression in the dorsal CA1 region of the hippocampus following contextual fear conditioning

We previously found that RPT6 has an epigenetic role in memory formation, which is independent of its role in the proteasome (Jarome et al., 2021), though the gene targets of RPT6 following learning remain unknown. To determine the gene targets of RPT6 during fear memory formation, we infused either Scr-siRNA (control) or siRNA targeting *Psmc5*, the RPT6-coding gene, into the dorsal CA1 region of the hippocampus in male rats and then trained them to a contextual fear paradigm 5 d later. One hour after training, rats were euthanized, brains were removed, CA1 tissue was isolated, and RNA was collected for RNA-seq (Fig. 1*A*). Female animals were not included due to the necessity of proteasome activity in the hippocampus of females, but not males, for memory formation, which could be impacted by *Psmc5* knockdown and complicate interpretation of the role of free RPT6 (Martin et al., 2021). In separate (all naïve) animals, we confirmed that our siRNA could effectively reduce *Psmc5* gene expression at 5 d post-infusion (two-tailed *t* test, $t_9 = 8.312$, $p < 0.0001$, $n = 5$–6 per group). In our RNA-seq analysis, we identified 46 differentially expressed genes following training in the Scr-siRNA trained group compared to Scr-siRNA naïve animals (Fig. 1*C*), but only 20 differentially expressed genes were identified following training in the *Psmc5*-siRNA trained animals (Fig. 1*D*), indicating that RPT6 regulates expression of at least 26 genes following learning. We next wanted to take a closer look at the direction of expression following training to determine if RPT6 is involved in upregulation or downregulation of target genes (Table 1). We first compared genes with

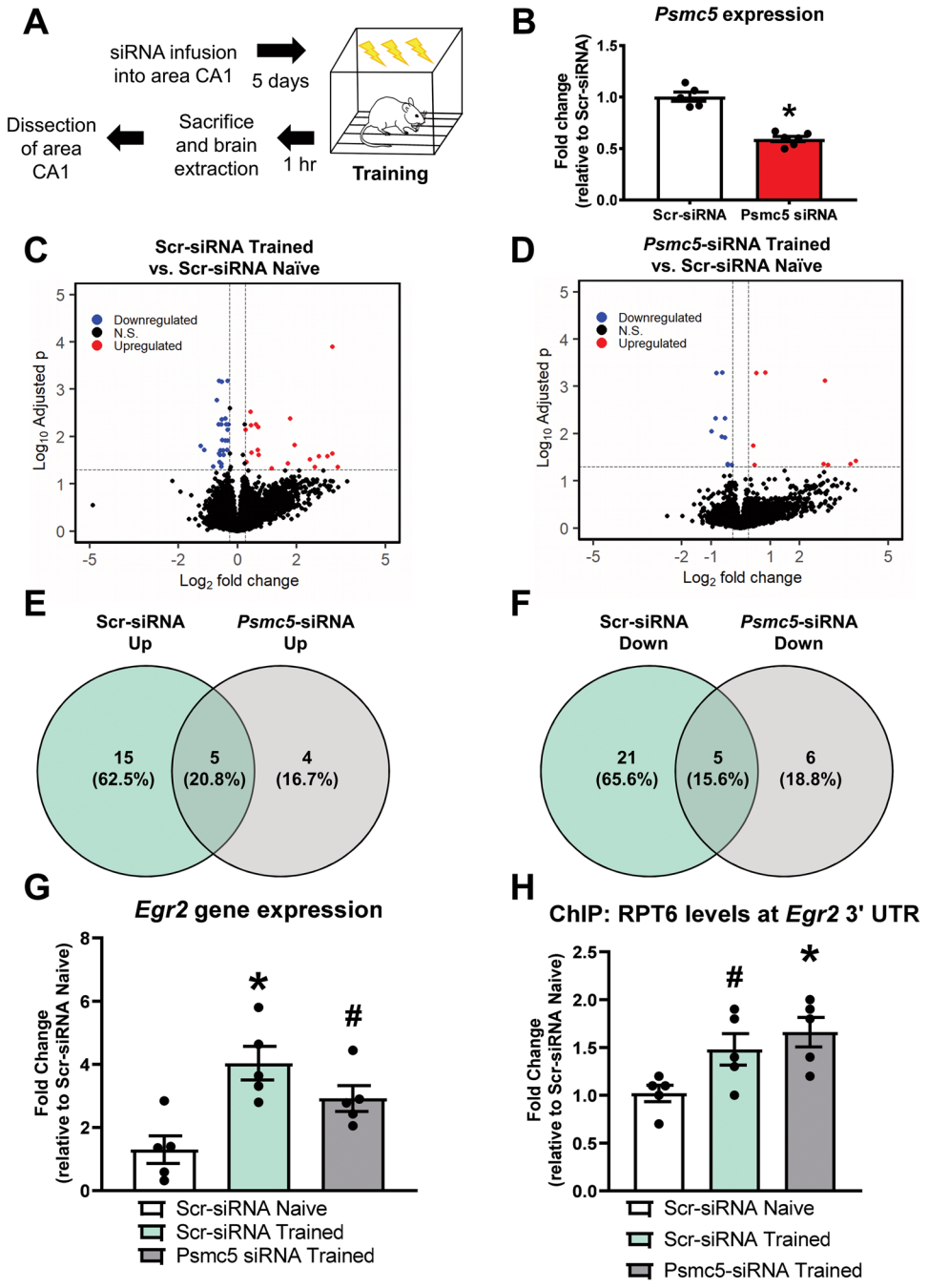

Figure 1. RNA-sequencing analysis reveals RPT6 regulates both upregulation and downregulation of target genes during memory formation in the CA1 region of male rats. ***A***, Male rats received a bilateral infusion of either nontargeting control (Scr-siRNA) Accell siRNA or Accell siRNA targeting *Psmc5*, the coding gene for RPT6, into area CA1 of the dorsal hippocampus. Five days after the siRNA infusion, rats in a training group were trained to standard contextual fear conditioning and then euthanized 1 h later, with naïve rats being euthanized at a similar timepoint. The CA1 region of the dorsal hippocampus was dissected, RNA was collected, and RNA-sequencing was conducted. ***B***, Confirmation of successful *Psmc5* knockdown in naïve animals using our siRNA approach. ***C***, ***D***, Volcano plot of RNA-seq expression data in the CA1 region of the hippocampus of Scr-siRNA trained compared to naïve (***C***) and *Psmc5*-siRNA trained compared to naïve (***D***) 1 h after context fear conditioning. Upregulated or downregulated genes are represented as red or blue, respectively, and nondifferentially expressed genes (DEGs) are represented as black. The dotted lines indicate the thresholds for DEG criteria. ***E***, ***F***, Venn diagrams showing number of genes upregulated (***E***) or downregulated (***F***) in Scr-siRNA trained group compared to *Psmc5*-siRNA trained group. ***G***, *Egr2* expression was increased in trained animals that received the Scr-siRNA, but not *Psmc5*-siRNA, compared to naïve animals that received Scr-siRNA. ***H***, Chromatin immunoprecipitation revealed increased RPT6 levels at *Egr2* in trained animals that received *Psmc5* targeting siRNA, but not animals that receive Scr-siRNA, compared to Scr-siRNA naïve. *$p < 0.05$ from Scr-siRNA naïve. **$p < 0.1$ from Scr-siRNA naïve in Tukey's HSD *post hoc* test.

upregulation following training in Scr-siRNA and *Psmc5*-siRNA animals and found that 20 and 9 genes, respectively, were upregulated but that only 5 genes were upregulated in both groups (Fig. 1*E*). Conversely, 26 and 11 genes were downregulated in Scr-siRNA and *Psmc5*-siRNA animals, respectively, following training, and again only 5 genes were downregulated in both groups (Fig. 1*F*). Importantly, these data provide the first evidence that RPT6 regulates both upregulation and downregulation of genes in area CA1 of the hippocampus following learning, as it has been previously shown that RPT6 works as a

Table 1. Comparison of DEGs during contextual memory formation in the dCA1 region of the hippocampus of male *Psmc5*-siRNA trained animals and Scr-siRNA trained animals

Scr-siRNA	Both	Psmc5-siRNA
Upregulated genes		
Hmox1	AC125248.1	Ms4a4e
Spp1	Fxyd2	AABR07038983.1
LOC24906	Per1	Scimp
S100a9	Tubb2b	Ccdc117
Timp1	Ddit4	-
Ermap	-	-
Egr2	-	-
Ckap2l	-	-
Fmo3	-	-
Ybx1-ps3	-	-
Irf9	-	-
Junb	-	-
B3gnt2	-	-
Pno1	-	-
Ran	-	-
Downregulated genes		
AABR07007032.1	Kdr	Egln3
AABR07018857.1	Tnfrsf11b	Col4a4
RGD1565616	Slc22a8	RGD1561113
Capn5	Clec14a	Bcam
Plcl1	Dll4	Mansc1
Ptprd	-	Edn1
Enpp1	-	-
Gprc5b	-	-
Bach2	-	-
Pls1	-	-
Spock1	-	-
Tmc7	-	-
Pcsk5	-	-
Fzd6	-	-
Slc6a7	-	-
Antxr1	-	-
Zmynd12	-	-
Tnfsf10	-	-
Susd5	-	-
Tmem215	-	-
Smyd1	-	-

binding partner of H2BubiK120 to establish trimethylation of histone H3 at lysine 4 (H3K4me3), leading to upregulation of the c-*fos* gene (Jarome et al., 2021).

We next wanted to investigate how RPT6 DNA binding regulates gene expression, so we chose a target gene to evaluate expression following *Psmc5* knockdown. Immediate early genes (IEGs) are known to be upregulated following neuronal activity (Tischmeyer and Grimm, 1999). *Egr2*, an IEG which was previously reported to be upregulated following contextual fear conditioning (Duke et al., 2017), was identified as being a target of RPT6 in our RNA-seq analysis. Therefore, we chose *Egr2* as our target gene to evaluate the role of RPT6 DNA binding in regulation of gene expression. We first confirmed with qRT-PCR that *Egr2* expression was upregulated in Scr-siRNA trained (one-way ANOVA, $F_{(2, 12)} = 8.836$, $p = 0.0044$, $n = 5$ per group; Tukey's HSD *post hoc* test $p = 0.0034$), but not *Psmc5*-siRNA trained (Tukey's HSD *post hoc* test, $p = 0.0700$), animals compared to Scr-siRNA naïve rats as indicated by the aforementioned RNA-Seq results (Fig. 1*G*). However, *Psmc5* knockdown did not completely prevent learning-induced increases in *Egr2* expression as there was a trend for higher *Egr2* levels in the *Psmc5* knockdown animals, which likely reflects that RPT6 is not solely responsible for *Egr2* upregulation during memory formation. Next, we conducted ChIP to identify where RPT6 was bound at various regions of *Egr2*, including, but not limited to, the promoter, Exon 1, and Exon 2 (data not shown). The 3′ untranslated region (UTR) of *Egr2* was the only region where significant changes in RPT6 levels 1 h after contextual fear conditioning (one-way ANOVA, $F_{(2, 12)} = 5.596$, $p = 0.0192$, $n = 5$ per group) were identified (Fig. 1*H*). Interestingly, although increased *Egr2* expression was not observed 1 h following training in the *Psmc5* knockdown group, the level of RPT6 bound to the 3′ UTR region of *Egr2* was significantly higher in the *Psmc5* knockdown group compared to control naïve animals (Tukey's HSD *post hoc* test, $p = 0.0179$). These data indicate that despite the downregulation of *Psmc5* and corresponding changes in *Egr2* expression, RPT6 levels at *Egr2* remain elevated.

Artificial placement of RPT6 at *Egr2* in the dorsal hippocampus may affect gene expression following weak contextual fear conditioning

After identifying a role for RPT6 in the regulation of gene expression during memory formation in area CA1, we next wanted to determine if the presence of RPT6 alone at a gene was sufficient to drive changes in expression. To investigate this, we first developed a method for artificially placing RPT6 at a gene by creating a CRISPR-dCas9-RPT6 fusion protein which allowed us to drive RPT6 to our target location (*Egr2*) through recruitment of the fusion protein with a gRNA. The fusion protein codes for dCas9, the endogenous *Rattus norvegicus* RPT6, and a 3× FLAG label, which was added to visualize expression and ensure the plasmid was translated correctly (Fig. 2*A*). We validated the expression of the plasmid in the dorsal CA1 region of the hippocampus, which showed stable expression 28 d after infusion with in vivo JetPEI transfection reagent (Fig. 2*B*). After confirming stable plasmid expression, we employed the dCas9-RPT6-FLAG plasmid to place RPT6 at the *Egr2* promoter. Animals received a bilateral infusion of either *Egr2* gRNA plasmid alone (control) or *Egr2* gRNA with the dCas9-RPT6-FLAG plasmid (*Egr2* + dCas9-RPT6) into the dorsal CA1 region of the hippocampus of male rats. After 28 d, animals were trained to a weak contextual fear paradigm, which we previously found does not lead to recruitment of RPT6 to c-*fos* or robust memory formation (Jarome et al., 2021), euthanized 1 h later, and then CA1 tissue was collected (Fig. 2*C*). Although animals underwent weak training, *Egr2* expression was significantly increased in control trained (one-way ANOVA, $F_{(2, 19)} = 25.64$, $p \leq 0.0001$, $n = 7–8$ per group; Tukey's HSD *post hoc* test, $p = 0.0002$) and *Egr2* + dCas9-RPT6 trained rats (Tukey's HSD *post hoc* test, $p < 0.0001$) compared to control naïve animals, although the magnitude of significance was larger in *Egr2* + dCas9-RPT6 trained animals (Fig. 2*D*). This larger magnitude of significance suggests that RPT6 placement at DNA alone may exert an effect on transcription, but the large and unexpected increase in *Egr2* expression following weak training makes a conclusive interpretation difficult. We next wanted to detect our dCas9-RPT6-FLAG protein at DNA, but the 3× FLAG antibody was not suitable for ChIP, so we used the RPT6 antibody instead to conduct ChIP. We observed significantly lower levels of RPT6 in the *Egr2* promoter region of control trained rats compared to control naïve animals (one-way ANOVA, $F_{(2, 19)} = 3.576$, $p = 0.0481$, $n = 7–8$ per group; Tukey's HSD *post hoc* tests, $p = 0.0388$), but no differences in the *Egr2* + dCas9-RPT6

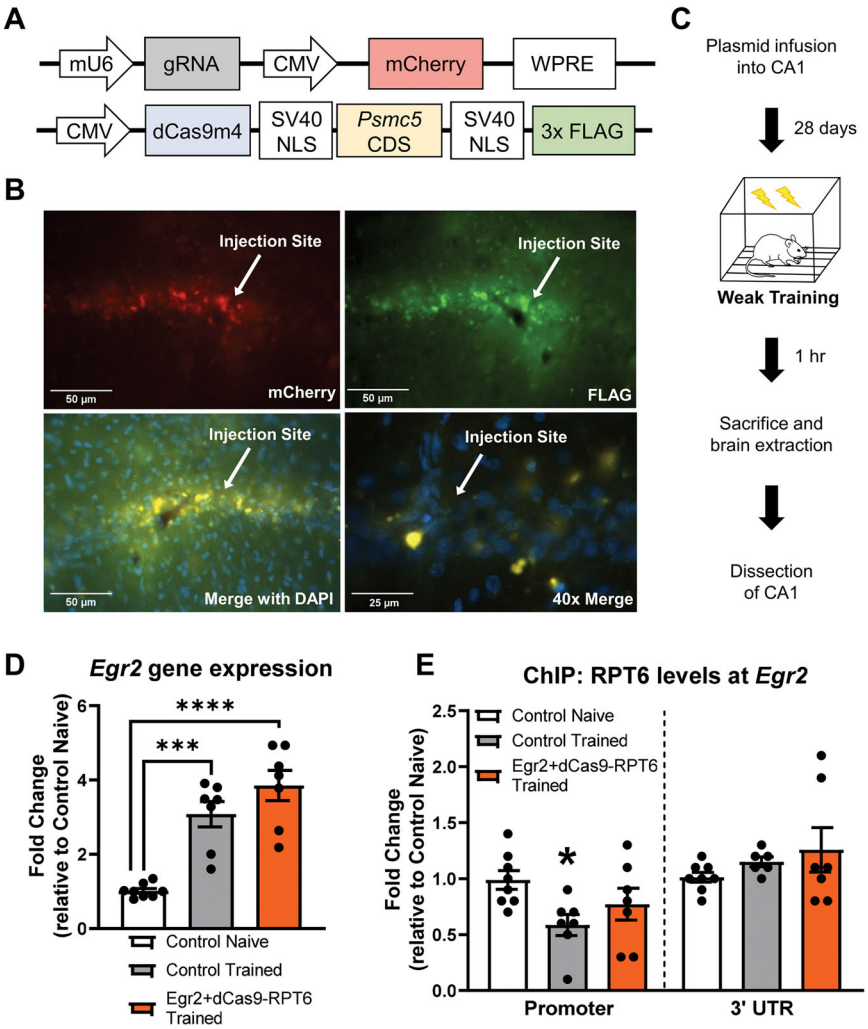

Figure 2. Artificially placing RPT6 at the *Egr2* promoter drives expression after weak contextual fear conditioning in the CA1 region of male rats. ***A***, Schematic of plasmid constructs, with the top showing construct of the dCas9-gRNA plasmid and the bottom showing our custom dCas9-RPT6-FLAG fusion plasmid. ***B***, Immunofluorescent image showing 20× images of CRISPR gRNA expression (red; top left) and 3× FLAG expression (green; top right) in the CA1 region of the hippocampus 28 d after plasmid infusion. Merged images of 3× FLAG, CRISPR gRNA, and DAPI are shown at 20× magnification (bottom left) and 40× magnification (bottom right). ***C***, Male rats received a bilateral infusion of either *Egr2* gRNA alone (control) or *Egr2* gRNA with the CRISPR-dCas9-RPT6-FLAG plasmid (*Egr2* + dCas9-RPT6) into area CA1 of the dorsal hippocampus. After 28 d, rats were trained to a weak contextual fear conditioning, euthanized 1 h later, and then the CA1 region of the dorsal hippocampus was collected. ***D***, *Egr2* expression was increased in control trained and *Egr2* + dCas9-RPT6 trained animals following weak training compared to control naïve animals. The magnitude of significance was larger in *Egr2* + dCas9-RPT6 trained animals, as indicated by Tukey's HSD *post hoc* test. ***E***, Chromatin immunoprecipitation of RPT6 revealed decreased levels of RPT6 at the *Egr2* promoter of control trained rats compared to control naïve rats, but no difference in RPT6 levels at the 3′ UTR region of *Egr2*. *$p < 0.05$, ***$p < 0.001$, ****$p < 0.0001$ from control naïve.

animals compared to control naïve (Tukey's HSD *post hoc* test, $p = 0.3444$) or control trained animals (Tukey's HSD *post hoc* test, $p = 0.4716$; Fig. 2*E*). Additionally, we did not observe any changes in RPT6 levels at the 3′ UTR of *Egr2* (one-way ANOVA, $F_{(2, 18)} = 1.116$, $p = 0.3492$, $n = 7$–8 per group), where we previously saw changes following standard training procedures. The lack of weak training-induced significant decreases in RPT6 bound to the *Egr2* promoter in animals that received the dCas9-RPT6 plasmid indicates that driving RPT6 to the promoter via our dCas9-RPT6-FLAG plasmid partially rescues the loss of RPT6 that normally occurs following weak training. Together, these data demonstrate that driving RPT6 to the promoter of *Egr2* may exert an effect on *Egr2* expression, but it is difficult to determine conclusively due to the unexpected upregulation of *Egr2* in control trained animals.

Phosphorylation of serine 120 of RPT6 is necessary for RPT6 to bind DNA and regulate gene expression in the dorsal hippocampus during fear memory formation

It has been shown that pRPT6-S120 is necessary for increases in proteasome activity (Zhang et al., 2007; Djakovic et al., 2009; Scudder et al., 2021), though whether this is needed for DNA binding is unknown. To test this, we used the CRISPR-dCas13-ADAR2DD RNA editing system to alter serine at position 120 on RPT6 to glycine (Fig. 3*A*). We designed a gRNA against *Psmc5* targeting S120 and tested it in vitro using B35 rat neuroblastoma cells to determine its efficiency (Fig. 3*B*). After determining that the gRNA could successfully decrease pRPT6-S120 levels in vitro (one-tailed nonparametric Mann–Whitney test, $U = 12$, $p = 0.0361$, $n = 7$–8 per group), we infused the gRNA and dCas13b-ADAR2DD plasmids (RPT6 + Cas13) or dCas13-ADAR2DD alone (control) into area CA1 of the hippocampus

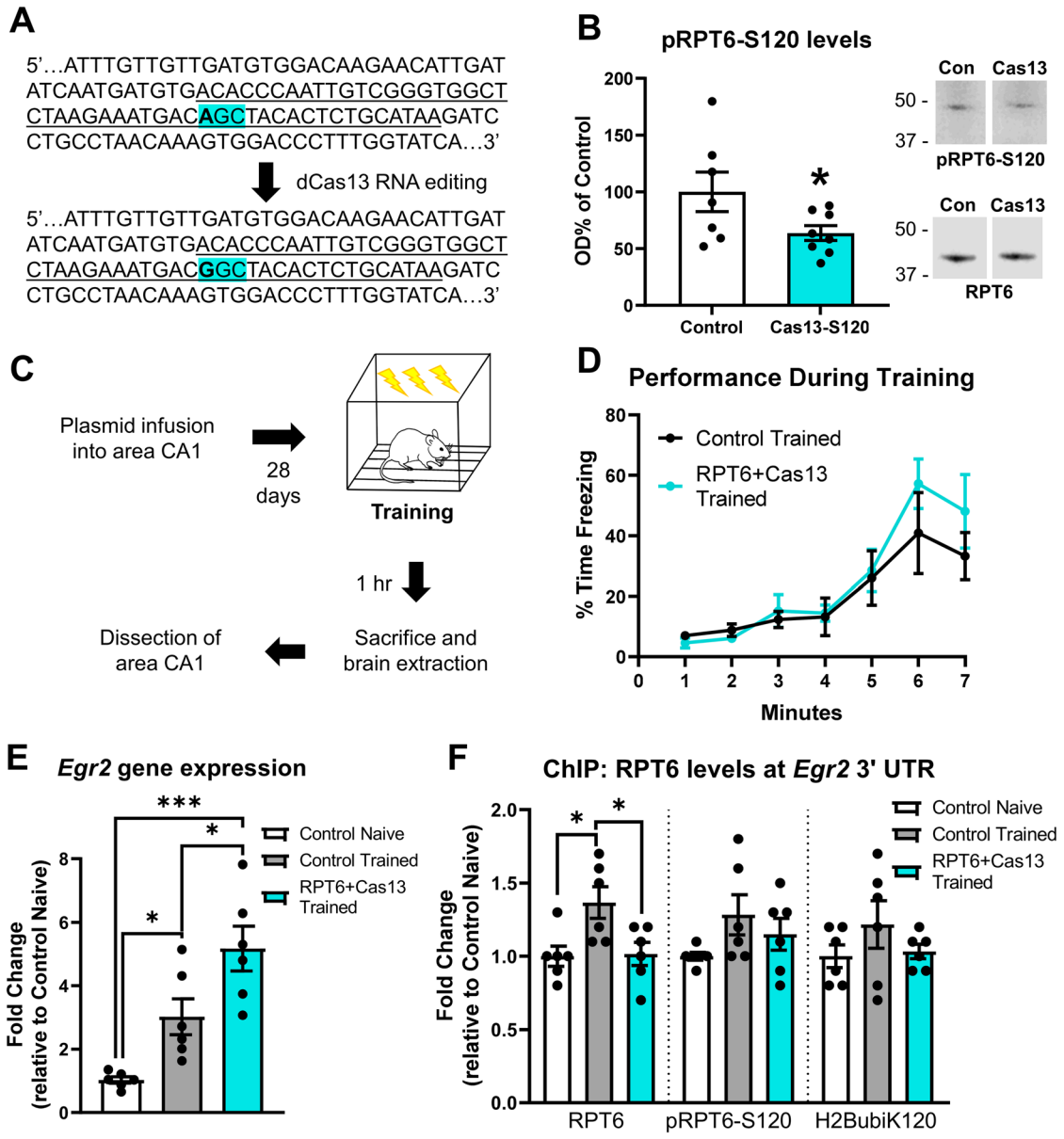

Figure 3. The serine 120 (S120) codon is necessary in the CA1 region of male rats for RPT6 to bind DNA following context fear conditioning. ***A***, The CRISPR-dCas13b-ADAR2DD RNA editing system was used to target the adenosine (bold) in the sequence coding for serine 120 (S120; highlighted blue). A 50 bp gRNA (indicated by underlined sequence) was generated against the RPT6-coding gene, *Psmc5*, mRNA sequence with a mismatch at the position 34 targeting adenosine. ***B***, The gRNA plasmid targeting S120 with the dCas13b-ADAR2DD plasmid (Cas13-S120) or dCas13b-ADAR2DD plasmid alone (control) were transfected into rat B35 neuroblastoma cells and then collected 48 h later. Western blot analysis revealed that pRPT6-S120 levels normalized to total RPT6 were downregulated. In representative Western blot images, the top box is pRPT6-S120 levels, and the bottom box is total RPT6 levels. ***C***, Male rats received a bilateral infusion of either gRNA targeting S120 and dCas13b-ADAR2DD plasmids (RPT6 + Cas13 trained) or dCas13b-ADAR2DD plasmid alone (control) into area CA1 of the dorsal hippocampus. After 28 d, rats were trained to standard contextual fear conditioning, euthanized 1 h later, and then the CA1 region of the dorsal hippocampus was collected. ***D***, Altering S120 of RPT6 through dCas13 targeting did not impact performance during training. ***E***, *Egr2* expression was significantly different between all. Both control trained and RPT6 + Cas13 trained animals had increased expression compared to control naïve rats, and animals in the RPT6 + Cas13 trained group also had increased expression compared to control trained animals. ***F***, Chromatin immunoprecipitation revealed increases in RPT6 bound to the 3′ UTR of *Egr2* in control trained animals compared to control naïve and RPT6 + Cas13 trained animals. There were no significant differences in levels of phosphorylation at S120 of RPT6 (pRPT6-S120) or monoubiquitination of histone H2B at lysine 120 (H2BubiK120). $*p < 0.05$ and $***p = 0.0001$.

then allowed 28 d for the plasmids to express, edit RNA, and then that edited RNA be translated into RPT6 protein lacking the phosphorylation site at S120. After 28 d, animals were trained to standard contextual fear conditioning, brains were collected 1 h later, and then area CA1 was dissected (Fig. 3*C*). The removal of S120 on RPT6 in the CA1 region of the hippocampus of males did not impact performance during the training session (two-way ANOVA, Time: $F_{(6, 60)} = 17.39$, $p \leq 0.0001$; Group: $F_{(1, 10)} = 0.5284$, $p = 0.4839$; Interaction: $F_{(6, 60)} = 0.9293$, $p = 0.4807$, $n = 6$ per group), as both groups performed similarly (Fig. 3*D*). To better understand the role of pRPT6-S120 in DNA binding and regulation of gene expression, we examined *Egr2* expression and RPT6, pRPT6-S120, and H2BubiK120 binding at the 3′ UTR of *Egr2*. *Egr2* expression was significantly increased (one-way ANOVA, $F_{(2, 15)} = 15.53$, $p = 0.0002$, $n = 6$ per group) in both control trained (Tukey's HSD *post hoc* tests, $p = 0.0424$) and RPT6 + Cas13 trained (Tukey's HSD *post hoc* tests, $p = 0.0001$) animals compared to control naïve, but RPT6 + Cas13 trained animals

also had significantly higher *Egr2* expression in the CA1 area compared to control trained animals (Tukey's HSD *post hoc* tests, $p = 0.0286$; Fig. 3*E*). Interestingly, ChIP analysis revealed increased binding of RPT6 at the 3′ UTR of *Egr2* in control trained animals compared to control naïve (one-way ANOVA with Tukey's HSD *post hoc* tests, $F_{(2, 15)} = 5.660$, $p = 0.0147$, $n = 6$ per group; Tukey's HSD *post hoc* tests, $p = 0.0240$), which was abolished in RPT6 + Cas13 trained animals (Tukey's HSD *post hoc* tests, $p = 0.0312$; Fig. 3*F*). Levels of pRPT6-S120 (one-way ANOVA, $F_{(2, 15)} = 1.917$, $p = 0.1814$, $n = 6$ per group) and H2BubiK120 (one-way ANOVA, $F_{(2, 15)} = 1.176$, $p = 0.3354$, $n = 6$ per group) bound to the 3′ UTR of *Egr2* were also measured, but there were no significant differences between groups. Together, these data indicate that phosphorylation of S120 is necessary for RPT6 to bind DNA and properly regulate gene expression in area CA1.

To better understand the relationship between RPT6 DNA binding and gene expression, we conducted simple linear regressions across all experiments (including the weak training) for each treatment with RPT6 bound at the 3′ UTR of *Egr2* as the independent variable and *Egr2* expression as the dependent variable. We first looked at control naïve animals across all experiments and observed a trend for a negative correlation (Simple Linear Regression, $R^2 = 0.2003$, $F_{(1, 16)} = 4.009$, $p = 0.0625$, $n = 18$–19 per group; Fig. 4*A*). Next, we looked at control trained animals, but we did not observe a correlation between RPT6 DNA levels and *Egr2* expression 1 h after training (Simple Linear Regression, $R^2 = 0.03786$, $F_{(1, 14)} = 0.5509$, $p = 0.4702$, $n = 17$ per group; Fig. 4*B*). Surprisingly, when we collapsed treatment (siRNA, dCas9, and dCas13) across all experiments (standard and weak training), we observed a strong negative correlation (Simple Linear Regression, $R^2 = 0.4020$, $F_{(1, 15)} = 10.08$, $p = 0.0063$, $n = 17$–18 per group) in trained animals that received a treatment impacting RPT6 (Fig. 4*C*), suggesting that any manipulation of RPT6 DNA binding activity resulted in an inverse impact on *Egr2* expression. Even more interesting is the similarity to the correlation for control naïve animals, where we observed a trend for the same inverse relationship. Together, these results suggest that *Egr2* expression cannot be predicted based on RPT6 DNA binding activity following training in control animals, but when RPT6 is manipulated prior to training, *Egr2* expression can be predicted to follow an inverse pattern with RPT6 levels at the 3′ UTR of *Egr2*.

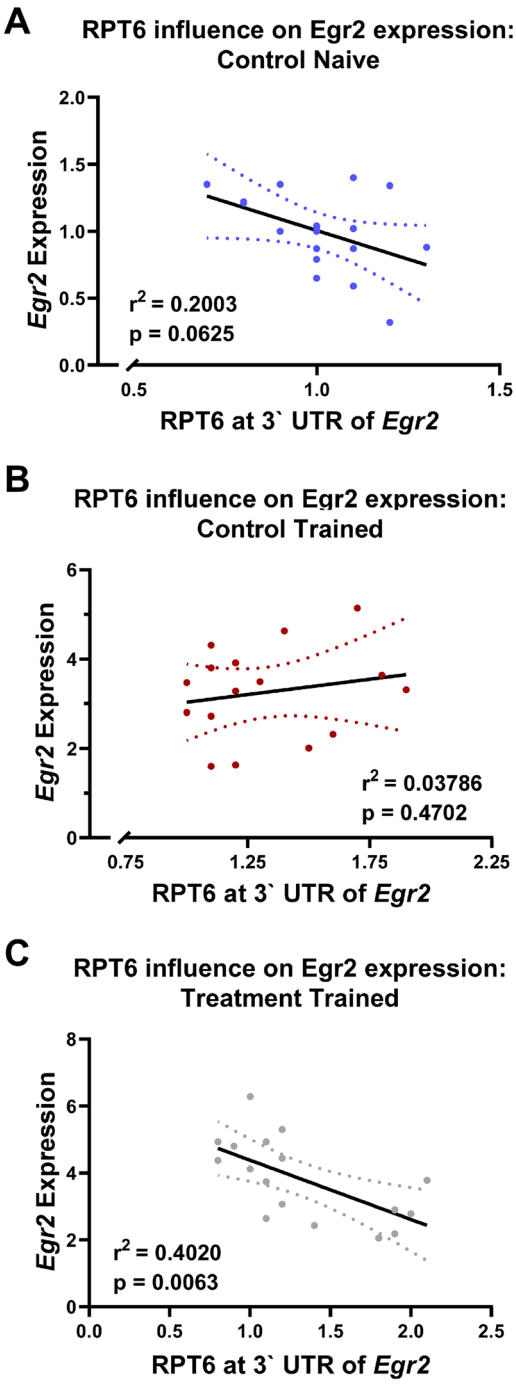

Figure 4. Manipulation of RPT6 leads to a negative correlation with *Egr2* expression. A simple linear regression was conducted to identify potential correlations between RPT6 bound at the 3′ UTR of *Egr2* (independent variable) and *Egr2* expression (dependent variable). To calculate correlation, we collapsed animals across all three experiments (siRNA, CRISPR-dCas9, and CRISPR-dCas13) within each group (control naïve, control trained, or treatment trained). ***A***, There was a trend for a negative correlation in control naïve animals across all experiments. ***B***, No significant correlation was observed in control trained animals across all experiments. ***C***, Trained animals that received a manipulation targeting RPT6 (siRNA knockdown, dCas9-mediated gene placement, or dCas13 targeting of S120) had a significant negative correlation, suggesting that disruption of homeostatic RPT6 levels/activity leads to dysregulated *Egr2* expression following training.

Phosphorylation of serine 120 of RPT6 is not necessary for memory formation in the dorsal hippocampus of male rats

After observing the loss of RPT6 bound at the 3′ UTR of *Egr2* following training in animals that received the dCas13 plasmids targeting S120, we wanted to investigate the role of pRPT6-S120 in memory formation. To determine if pRPT6-S120 is necessary for memory formation in the CA1 of the hippocampus, we injected the same plasmids into area CA1 of the hippocampus, waited 28 d, trained all animals to standard contextual fear conditioning, tested memory retention after 1 d, and then collected tissue and dissected out area CA1 of the hippocampus (Fig. 5*A*). As we previously observed, the S120 manipulation did not impact performance during the training session (two-way ANOVA, Time: $F_{(6, 84)} = 35.15$, $p \leq 0.0001$; Group: $F_{(1, 14)} = 0.3366$, $p = 0.5710$; Interaction: $F_{(6, 84)} = 0.5627$, $p = 0.7588$, $n = 8$ per group; Fig. 5*B*). Unexpectedly, the manipulation also had no impact on fear memory retention (two-tailed t test, $t_{(14)} = 0.2767$, $p = 0.7860$, $n = 8$ per group; Fig. 5*C*). Due to the previously reported importance of pRPT6-S120 for proteasome activity, we measured chymotrypsin-like (two-tailed nonparametric Mann–Whitney test, $U = 22$, $p = 0.3282$, $n = 8$ per group), peptidyl-glutamyl (two-tailed t test, $t_{(14)} = 0.9718$, $p = 0.3476$, $n = 8$ per group), and trypsin-like proteasome activity (two-tailed t test, $t_{(14)} = 0.9365$, $p = 0.3649$, $n = 8$ per group), but we found no differences

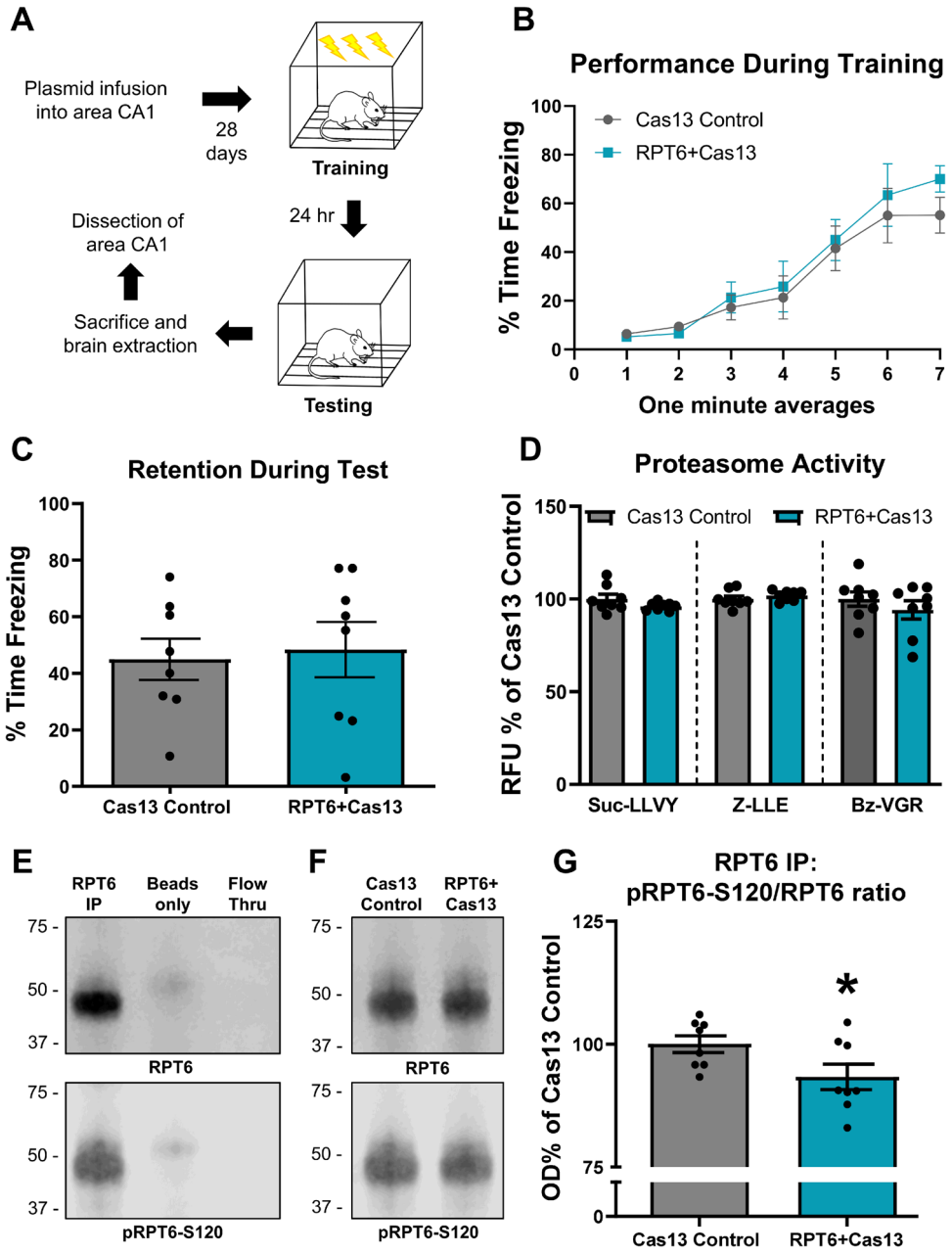

Figure 5. The serine 120 (S120) codon is not necessary for context fear memory formation in the CA1 region of male rats. ***A***, Male rats received a bilateral infusion of either gRNA targeting S120 and dCas13b-ADAR2DD plasmids (RPT6 + Cas13) or dCas13b-ADAR2DD plasmid alone (Cas13 control) into area CA1 of the dorsal hippocampus. After 28 d, rats were trained to standard contextual fear conditioning and then tested 24 h later. ***B***, ***C***, dCas13 targeting of S120 did not impact performance during training (***B***) nor did it alter memory retention during testing (***C***). ***D***, Proteasome activity measured in samples collected 1 h after testing was not different between groups for Suc-LLVY chymotrypsin-like, Z-LLE peptidyl-glutamyl or Bz-VGR trypsin-like activity. ***E***, Immunoprecipitation (IP) of RPT6 using CA1 whole-cell extract was completed to confirm knockdown of phosphorylation at serine 120 of RPT6 (pRPT6-S120). ***F***, Representative image of IP of RPT6 from CA1 whole-cell extract of Cas13 control and RPT6 + Cas13 trained animals for quantitative comparison with RPT6 in the top image and pRPT6-S120 in the bottom image. ***G***, The ratio of pRPT6-S120 levels to precipitated RPT6 levels was higher in Cas13 control animals compared with RPT6 + Cas13 animals confirming the knockdown of pRPT6-S120. $*p < 0.05$ compared to Cas13 control.

between groups (Fig. 5*D*). To confirm the CRISPR-dCas13 manipulation caused a knockdown of pRPT6-S120, we conducted an immunoprecipitation (IP) of RPT6 from whole-cell CA1 extracts of Cas13 control and RPT6 + Cas13 animals (Fig. 5*E*). We quantified RPT6 and pRPT6-S120 levels in our IP samples to compare phosphorylation levels between our groups (Fig. 5*F*). To account for potential variability of total RPT6 levels in our IP samples, we calculated a ratio of pRPT6-S120 to total immunoprecipitated RPT6 in each sample, which confirmed that pRPT6-S120 levels were lower in RPT6 + Cas13 animals compared to Cas13 control animals (two-tailed *t* test, $t_{(14)} = 2.153$, $p = 0.0492$, $n = 8$ per group; Fig. 5*G*). Together, these data suggest that pRPT6-S120 is not necessary for memory formation or baseline proteasome activity in the CA1 region of the hippocampus.

Discussion

Proteasome-independent RPT6 has been implicated in epigenetic regulation of gene expression in the hippocampus following

learning (Jarome et al., 2021), and pRPT6-S120 (within the proteasome) has been implicated in proteasome activity regulation (Zhang et al., 2007; Djakovic et al., 2009, 2012; Bingol et al., 2010), suggesting that RPT6 may have dual functions in the brain. Epigenetically, RPT6 works with H2BubiK120 to establish H3K4me3 (Ezhkova and Tansey, 2004; Jarome et al., 2021), though the gene targets of RPT6 and how it binds DNA remain unknown. Here, we characterize the transcriptional role of RPT6 in the dorsal hippocampus during fear memory formation and reveal the importance of the S120 phosphorylation site for DNA binding. Through RNA-seq, we identified a specific subset of differentially expressed genes regulated by RPT6 in the hippocampus during memory formation. Using our dCas9-RPT6-FLAG plasmid, we determined that RPT6 placement at DNA may be important for altering gene expression. Lastly, we altered S120 on RPT6 and determined that pRPT6-S120 is necessary for RPT6 to bind DNA and properly regulate gene expression following learning.

We report a specific transcriptional network regulated by RPT6 in the hippocampus of male rats during memory formation. RPT6 has been associated with transcriptional activation in the brain (Jarome et al., 2021) and both activation and repression in yeast (Ezhkova and Tansey, 2004; Lee et al., 2005), but this is the first report of RPT6-mediated transcriptional downregulation in the brain. Unfortunately, it remains unclear what molecules RPT6 works with (transcription factors, epigenetic marks) or if free RPT6 can work with proteasome functions to regulate clearance of transcription factors. However, some genes identified as being dysregulated by RPT6 knockdown have known roles in memory formation such as *Hmox1*, shown to be upregulated by a molecule that rescues fatigue-induced memory deficits (Bai et al., 2023). *Timp1* expression has been found to regulate hippocampus-dependent learning (Chaillan et al., 2006). Interestingly, *Tnfsf10* was downregulated in our dataset, and knockdown of *Tnfsf10* rescues cognitive deficits in hippocampus-dependent tasks in Alzheimer's disease mice (Cantarella et al., 2015). Together, we report RPT6 target genes with known roles in memory.

Using a unique CRISPR-dCas9-RPT6 plasmid to artificially place RPT6 at the *Egr2* promoter, we found that RPT6 presence at DNA alone may possibly exert an effect on transcription, but this was difficult to determine conclusively due to unexpected increases in *Egr2* expression following weak training. We previously found that this weak training protocol did not recruit RPT6 to DNA (Jarome et al., 2021). Here, weak training led to reduced endogenous RPT6 levels at the *Egr2* promoter, but the dCas9-RPT6-FLAG plasmid, which artificially placed RPT6 at the *Egr2* promoter, prevented the reduction in RPT6 levels. Our plasmids were efficiently transfected using in vivo JetPEI transfection reagent, but not all cells in the brain region were transfected, so a ratio of transfected and nontransfected cells was likely used in our ChIP assay and could have diluted the effects from this manipulation. In any case, considering that these data do not clearly show altered transcription due to RPT6 placement at *Egr2*, we did not test how memory could be affected by this manipulation. It is likely that driving RPT6 to *Egr2* alone may not be sufficient to induce robust memory formation, particularly because *Egr2* upregulation was occurring in the control trained animals and since weak training does not induce a robust memory.

To explore the role of pRPT6-S120 for RPT6 DNA binding, we altered the S120 site on RPT6 with CRISPR-dCas13 and found that RPT6 could no longer bind the 3′ UTR of *Egr2*, but *Egr2* expression was greatly enhanced, indicating that pRPT6-S120 is necessary for RPT6 DNA binding activity and proper regulation of gene expression. It seems counterintuitive that decreases in RPT6 binding to *Egr2* would lead to increased *Egr2* expression, however, siRNA-mediated knockdown of *Psmc5* increased RPT6 levels at *Egr2* and reduced *Egr2* expression, which follows an opposite pattern. As RPT6 is not a traditional transcription factor, it is unclear exactly how it regulates changes in transcription, but it is possible that it can work with a variety of molecules to properly regulate changes in gene expression.

The S120 phosphorylation site was not necessary for fear memory formation or baseline proteasome activity, suggesting that pRPT6-S120 is not necessary in the CA1 region for context memory formation. This is in line with another study which found that context fear memory was intact in phospho-dead mutant S120 knock-in mice (Scudder et al., 2021). This study did find diminished proteasome activity; however, this was likely because the knock-in approach would lead to S120 mutation in every cell in the body and the whole brain was used for analysis, as opposed to our hippocampus-specific analysis. It remains unclear how phosphorylation status dictates the epigenetic versus proteomic role of RPT6, but we can speculate that RPT6 could have unique functions in different cell types. For example, RPT6 has been implicated in regulating major histocompatibility complex class II (MHC-II) gene expression (Inostroza-Nieves et al., 2012), and one study found that *Egr2* and *Spp1*, two genes no longer upregulated following RPT6 knockdown in our dataset, were upregulated in MHC-II+ microglia (Yin et al., 2017), suggesting that pRPT6-S120 may regulate gene expression in glial cells, but control protein degradation in neurons. As pRPT6-S120 levels have been correlated with proteasome activity in other brain regions for different memory types (Jarome et al., 2013; Beamish et al., 2022), future studies should focus on identifying the necessity of pRTP6-S120 for other memory types and its proteomic and epigenetic roles in different brain regions.

In our prior study, we found H2BubiK120 and RPT6 bound at the same DNA regions following fear conditioning. As mentioned above, manipulation of S120 on RPT6 abolished its ability to bind *Egr2* and regulate proper gene expression, but we did not observe any significant changes in H2BubiK120 or pRPT6-S120 levels at *Egr2*. This is not necessarily surprising though, as the anti-pRPT6-S120 antibody is not ChIP-grade (one does not exist to our knowledge), so it is entirely possible that pRPT6-S120 levels were impacted but could not be detected through ChIP. Additionally, RPT6 has been shown to interact with acetylated histone H3 (Lee et al., 2005; Koues et al., 2009), suggesting that RPT6 may bind to epigenetic marks beyond just H2BubiK120. To determine the full extent of the epigenetic role of RPT6 in the hippocampus during memory formation, future studies should conduct RNA-seq in conjunction with ChIP-sequencing for RPT6 and various epigenetic modifications at different time points during memory formation in males and females following *Psmc5* knockdown.

To better understand the relationship between RPT6 DNA levels and gene expression, we collapsed experiments and conducted simple linear regression within each group to compare RPT6 levels at the 3′ UTR of *Egr2* and *Egr2* expression. Animals in the control naïve groups had a trend for a negative correlation. Animals in the control trained groups had no correlation between RPT6 levels and gene expression, suggesting that RPT6 binding to *Egr2* is not a good predictor of *Egr2* expression following training. Surprisingly, after collapsing treatments (*Psmc5*-siRNA, dCas9-RPT6 plasmids, or RPT6 + Cas13 plasmids), we observed

a significant negative correlation. Considering our manipulations had different effects on RPT6 DNA binding (siRNA knockdown caused increases, but RPT6 + Cas13 caused decreases in RPT6 levels at 3′ UTR of *Egr2*), this significant correlation suggests that naturally occurring endogenous RPT6 levels are necessary for proper DNA binding and gene regulation following training. This notion is supported by other studies that report knockdown and overexpression of RPT6 (Ferry et al., 2009) or proteasome inhibition and RPT6 overexpression (Zhu et al., 2004) leads to decreased transcription of target genes. Therefore, it would be interesting to investigate the impact of proteasome inhibitors on transcription of RPT6 target genes.

We previously identified RPT6 bound to H2BubiK120 in the hippocampus of female rats following learning (Farrell et al., 2022), though the present study used only male rats. This is because females, but not males, require functional proteasome activity in the hippocampus for memory formation (Martin et al., 2021), complicating the interpretation of the role of free RPT6 in the hippocampus of females. We can speculate that because females require proteasome activity in this region, RPT6 may work solely in the proteasome in the hippocampus of female rats. Alternatively, free RPT6 may play an epigenetic role in the hippocampus of females based on the evidence of it binding with H2BubiK120. We can hypothesize that in the female hippocampus, free RPT6 works similarly to its transcriptional role in males during memory formation, but ultimately more studies should be conducted to characterize the role of free versus proteasome-bound RPT6 in females.

Together, this study identifies RPT6 gene targets in the male hippocampus during memory formation, demonstrates that RPT6 alone at DNA may alter gene expression, and recognizes pRPT6-S120 as a regulator of RPT6 DNA binding. These results provide new insights into the complex role of proteasome-independent functions of the UPS during memory formation and demonstrate that dysregulation of RPT6 may lead to altered transcriptional profiles.

References

Bai L, Tan C, Ren J, Liu J, Zou W, Liu G, Sheng Y (2023) *Cordyceps militaris* acidic polysaccharides improve learning and memory impairment in mice with exercise fatigue through the PI3 K/NRF2/HO-1 signalling pathway. Int J Biol Macromol 227:158–172.

Beamish SB, Gross KS, Anderson MM, Helmstetter FJ, Frick KM (2022) Sex differences in training-induced activity of the ubiquitin proteasome system in the dorsal hippocampus and medial prefrontal cortex of male and female mice. Learn Mem 29:302–311.

Bingol B, Wang CF, Arnott D, Cheng D, Peng J, Sheng M (2010) Autophosphorylated CaMKIIalpha acts as a scaffold to recruit proteasomes to dendritic spines. Cell 140:567–578.

Bourtchouladze R, Abel T, Berman N, Gordon R, Lapidus K, Kandel ER (1998) Different training procedures recruit either one or two critical periods for contextual memory consolidation, each of which requires protein synthesis and PKA. Learn Mem 5:365–374.

Cantarella G, Di Benedetto G, Puzzo D, Privitera L, Loreto C, Saccone S, Giunta S, Palmeri A, Bernardini R (2015) Neutralization of TNFSF10 ameliorates functional outcome in a murine model of Alzheimer's disease. Brain 138:203–216.

Chaillan FA, Rivera S, Marchetti E, Jourquin J, Werb Z, Soloway PD, Khrestchatisky M, Roman FS (2006) Involvement of tissue inhibition of metalloproteinases-1 in learning and memory in mice. Behav Brain Res 173:191–198.

Cox DBT, Gootenberg JS, Abudayyeh OO, Franklin B, Kellner MJ, Joung J, Zhang F (2017) RNA editing with CRISPR-Cas13. Science 358:1019–1027.

Djakovic SN, Schwarz LA, Barylko B, DeMartino GN, Patrick GN (2009) Regulation of the proteasome by neuronal activity and calcium/calmodulin-dependent protein kinase II. J Biol Chem 284:26655–26665.

Djakovic SN, Marquez-Lona EM, Jakawich SK, Wright R, Chu C, Sutton MA, Patrick GN (2012) Phosphorylation of Rpt6 regulates synaptic strength in hippocampal neurons. J Neurosci 32:5126–5131.

Duke CG, Kennedy AJ, Gavin CF, Day JJ, Sweatt JD (2017) Experience-dependent epigenomic reorganization in the hippocampus. Learn Mem 24:278–288.

Ezhkova E, Tansey WP (2004) Proteasomal ATPases link ubiquitylation of histone H2B to methylation of histone H3. Mol Cell 13:435–442.

Farrell K, Auerbach A, Musaus M, Jarome TJ (2022) The epigenetic role of proteasome subunit RPT6 during memory formation in female rats. Learn Mem 29:256–264.

Farrell K, Musaus M, Auerbach A, Navabpour S, Ray WK, Helm RF, Jarome TJ (2023) Proteasome-independent K63 polyubiquitination selectively regulates ATP levels and proteasome activity during fear memory formation in the female amygdala. Mol Psychiatry 28:2594–2605.

Ferry C, Gianni M, Lalevée S, Bruck N, Plassat JL, Raska I Jr, Garattini E, Rochette-Egly C (2009) SUG-1 plays proteolytic and non-proteolytic roles in the control of retinoic acid target genes via its interaction with SRC-3. J Biol Chem 284:8127–8135.

Gonzalez F, Delahodde A, Kodadek T, Johnston SA (2002) Recruitment of a 19S proteasome subcomplex to an activated promoter. Science 296:548–550.

Hamilton AM, Oh WC, Vega-Ramirez H, Stein IS, Hell JW, Patrick GN, Zito K (2012) Activity-dependent growth of new dendritic spines is regulated by the proteasome. Neuron 74:1023–1030.

Hershko A, Ciechanover A (1998) The ubiquitin system. Annu Rev Biochem 67:425–479.

Inostroza-Nieves Y, Venkatraman P, Zavala-Ruiz Z (2012) Role of Sug1, a 19S proteasome ATPase, in the transcription of MHC I and the atypical MHC II molecules, HLA-DM and HLA-DO. Immunol Lett 147:67–74.

Jarome TJ, Kwapis JL, Ruenzel WL, Helmstetter FJ (2013) CaMKII, but not protein kinase A, regulates Rpt6 phosphorylation and proteasome activity during the formation of long-term memories. Front Behav Neurosci 7:115.

Jarome TJ, et al. (2021) Ubiquitination of histone H2B by proteasome subunit RPT6 controls histone methylation chromatin dynamics during memory formation. Biol Psychiatry 89:1176–1187.

Koues OI, Dudley RK, Mehta NT, Greer SF (2009) The 19S proteasome positively regulates histone methylation at cytokine inducible genes. Biochim Biophys Acta 1789:691–701.

Lander GC, Estrin E, Matyskiela ME, Bashore C, Nogales E, Martin A (2012) Complete subunit architecture of the proteasome regulatory particle. Nature 482:186–191.

Lee D, Ezhkova E, Li B, Pattenden SG, Tansey WP, Workman JL (2005) The proteasome regulatory particle alters the SAGA coactivator to enhance its interactions with transcriptional activators. Cell 123:423–436.

Martin K, Musaus M, Navabpour S, Gustin A, Ray WK, Helm RF, Jarome TJ (2021) Females, but not males, require protein degradation in the hippocampus for contextual fear memory formation. Learn Mem 28:248–253.

Melfi R, Cancemi P, Chiavetta R, Barra V, Lentini L, Di Leonardo A (2020) Investigating REPAIRv2 as a tool to edit CFTR mRNA with premature stop codons. Int J Mol Sci 21:4781.

Patrick MB, Omar N, Werner CT, Mitra S, Jarome TJ (2023) The ubiquitin-proteasome system and learning-dependent synaptic plasticity — a 10 year update. Neurosci Biobehav Rev 152:105280.

Scudder SL, Gonzales FR, Howell KK, Stein IS, Dozier LE, Anagnostaras SG, Zito K, Patrick GN (2021) Altered phosphorylation of the proteasome subunit Rpt6 has minimal impact on synaptic plasticity and learning. eNeuro 8:1–12.

Tischmeyer W, Grimm R (1999) Activation of immediate early genes and memory formation. Cell Mol Life Sci 55:564–574.

Weber Boutros S, Unni VK, Raber J (2022) An adaptive role for DNA double-strand breaks in hippocampus-dependent learning and memory. Int J Mol Sci 23:8352.

Yin Z, et al. (2017) Immune hyperreactivity of Aβ plaque-associated microglia in Alzheimer's disease. Neurobiol Aging 55:115–122.

Zhang F, Hu Y, Huang P, Toleman CA, Paterson AJ, Kudlow JE (2007) Proteasome function is regulated by cyclic AMP-dependent protein kinase through phosphorylation of Rpt6. J Biol Chem 282:22460–22471.

Zhu Q, Yao J, Wani G, Chen J, Wang QE, Wani AA (2004) The ubiquitin-proteasome pathway is required for the function of the viral VP16 transcriptional activation domain. FEBS Lett 556:19–25.